PHYSICAL REVIEW B VOLUME 27, NUMBER 2 15 JANUARY 1983

# Electronic structure of supported small metal clusters

M. G. Mason
*Research Laboratories, Eastman Kodak Company, Rochester, New York 14650*
(Received 26 August 1982)

Photoemission, Auger, and x-ray absorption spectroscopy have been used in a systematic study of small metal clusters on a variety of supports. The degree of cluster-support interaction for clusters of group-VIII and noble metals can be divided into two categories: supports with localized $p$ or $d$ orbitals with binding energies overlapping those of the cluster $d$ orbitals and supports without such orbitals. The first type is considered strongly interacting, whereas the latter type is only weakly interacting. For weakly interacting substrates such as carbon, the energy shifts in photoemission, Auger, and x-ray absorption edges, as well as changes in x-ray edge intensities, photoemission valence-orbital intensities and splittings, and photoemission and Auger linewidths all show that initial-state properties are much more sensitive to cluster size than are the final-state properties. The photoemission spectra of small clusters and those of alloys and intermetallic compounds are quantitatively compared. For weakly interacting substrates and host metals, the photoemission spectra of clusters and alloys are virtually identical, depending only on the average coordination number $\bar{n}$. In these systems the net interatomic charge transfer to the substrate or host atoms is very small. However, there is a significant intra-atomic charge transfer, which increases the $d$-electron count with increasing cluster size or alloy concentration. For strongly interacting supports, the cluster binding energy is usually shifted to lower binding energy. This shift can be understood from simple molecular-orbital arguments. The experimental conclusions are supported by calculations with the use of the thermodynamic model of Johansson and Mårtensson. Their model accurately predicts the observed binding-energy shifts and shows that initial-state effects dominate for weakly interacting systems and that final-state processes are relatively more important for the reactive substrates.

## I. INTRODUCTION

The electronic structure of small metal clusters has been an active area of research for both the theoretician[1] and the experimentalist.[2–19] This activity has been motivated primarily by the tremendous technological importance of metal clusters, particularly in heterogeneous catalysis.[20] To a somewhat lesser extent this research has been stimulated by a desire to understand the basic physics involved in the transition from the discrete energy levels of free atoms to the continuous, $k$-dependent energy bands of bulk metals.[16,17]

One of the most productive techniques in this area of research has been that of electron spectroscopy, particularly photoemission. It has been applied with considerable success to practical industrial catalysts; however, most of the basic understanding of the electronic properties of metal clusters has come from studies of more well-defined and controllable model systems. Particularly, the metal nuclei formed in the earliest stages of vapor deposition on well-characterized substrates[21–24] are ideal systems for study by modern techniques of surface analysis, including x-ray and ultraviolet photoelectron spectroscopy[2,4–7,10–19] (XPS and UPS), Auger electron spectroscopy[3,10,15] (AES), and transmission electron microscopy[20–24] (TEM). Amorphous carbon has been the most widely used substrate,[2,3,5–9,12–17,19–24] and the noble and group-VIII metals have been the most thoroughly studied metals.[2–14,20–24] Other substrates such as $SiO_2$,[6] $Al_2O_3$,[4] $SrTiO_3$,[10] alkali halides,[11] and organic polymers[18] have been used but much less than carbon. The general experimental results of these many studies are now well established. The core-level binding energies ($E_B$) generally decrease and the splitting or width of the valence $d$ bands increases with increasing size. Auger kinetic energies increase and the core orbital XPS and Auger linewidths decrease as the bulk metal is approached. These general characteristics are well accepted, but the physical origin of these spectral changes remains an area of considerable dispute. This paper presents experimental and theoretical results to help resolve some of the areas of contention. Section II briefly reviews the experi-

 

mental procedures. Section III considers initial versus final-state properties in determining the changes in photoemission spectra as the particle size varies. Section IV establishes the close similarity, in terms of photoemission, between clusters and alloys, and exploits this similarity to try to understand the electronic structure of clusters in terms of alloys. In Sec. IV the cluster-alloy relationship is extended further by use of a thermodynamic model[25] to more fully understand the electronic structure of clusters. Section V summarizes the conclusions of this work.

## II. EXPERIMENTAL

The XPS measurements were made on a Hewlett-Packard 5950A electron spectroscopy for chemical analysis (ESCA) spectrometer using Al $K\alpha$ radiation (1486.6 eV) with an energy resolution of better than 0.6 eV. Some x-ray-induced Auger electron spectra (AES) were also recorded on this instrument. The standard operating vacuum was less than $2\times10^{-9}$ Torr. Metal nuclei and metallic substrates were evaporated from resistive sources in the sample preparation chamber of the spectrometer. No carbon or oxygen contamination could be detected in the XPS spectra. Carbon and silica substrates were prepared in a separate chamber and cleaned in the spectrometer by argon-ion bombardment. When metallic substrates were used, either a substrate core level or the Fermi level was used for binding-energy ($E_B$) calibration. For the C and $SiO_2$ substrates the C 1$s$ or Si 2$p$ lines were normally used; on occasion the 2$p$ levels of residual implanted Ar were used as a calibration check. This line was sharper than the substrate carbon or silicon lines but was normally fairly weak. The coverage of the metal nuclei was routinely determined from core-level intensities relative to those of the substrate. These values were periodically checked by neutron-activation analysis.

The electron-excited Auger spectra were recorded on a conventional double-pass cylindrical mirror analyzer. The Auger energies were taken as the peak in the second-derivative spectra and were calibrated with respect to the $L_3M_3M_3$ line of residual argon. Metal coverages in these samples were determined by neutron activation.

The x-ray absorption measurements (XAS) were made on the focused extended x-ray absorption fine-structure (EXAFS) beam line II-4 at the Stanford Synchrotron Radiation Laboratory (SSRL) by standard techniques. Samples sufficiently concentrated for transmission x-ray absorption studies were formed by evaporating alternate layers of metal and carbon onto 4000-Å polymer films. The films were folded several times and stacked together.[9] Uniformity of particle size was achieved by controlling the amount of deposited material in each layer. For a typical sample, total equivalent thickness of Pd averaged $\sim0.4$ $\mu$m. XPS studies of similarly prepared layers of highly reactive nickel clusters overcoated with as little as 10 Å of carbon showed no signs of oxidation due to ambient exposure.

## III. CLUSTERS: INITIAL- AND FINAL-STATE EFFECTS

The quantity most often reported in XPS studies of metallic clusters is the shift in core- and valence-level binding energies with size. The general trend is for $E_B$ of the core levels to be high for the small clusters and to decrease to the bulk value as the number of cluster atoms increases. The shifts in the centroid of the valence $d$ band $\epsilon_d$ follow the same general trend, with the total shift being slightly less than that of the core levels.[26] Some of the observed core shifts are listed in Table I. Shifts using organic[18] and alkali halide[11] substrates have also been reported, but because of the lack of information on nucleation and growth in these materials, they will not be considered further.

This section presents the physical basis for binding-energy shifts in metal clusters. The possible origins of such shifts have been discussed in detail by Watson and co-workers.[27] Of the many factors considered, two have received the most attention for supported clusters of the type used in this study. The first observations of core-level shifts with cluster size were interpreted as resulting from a size dependence of the initial-state electronic structure.[14] Specifically, changes in the number of valence $d$ electrons with size were thought to be responsible for the observed shifts. Later work presented an alternative interpretation that the shifts in $E_B$ were, in fact, not due to the initial-state properties at all, but rather to variations in the final-state relaxation processes.[7,10] Data supporting each of these models are examined here, and new results are presented to show that final-state effects are of only minor importance on supports such as carbon and silica.

### A. Relaxation model

If an atom or a small cluster is considered as an isolated species, then it is clear that its core-level binding energies (even with appropriate correction for differences in reference levels) will be larger than those measured in the bulk metal. Much of this change is certainly due to the extra-atomic relaxation processes in the condensed state.[28] In the solid, the hole state produced by photoionization is shielded by the conduction electrons and the cores of neighboring atoms. This effect lowers the energy of the final state and results in a lower measured bind-

TABLE I. Core-level binding-energy shifts for various metals and substrates. Shift $\Delta E = E_B(\text{supported atom}) - E_B(\text{metal})$.

| Metal-substrate | Shift $\Delta E$ (eV) | Metal-substrate | Shift $\Delta E$ (eV) |
|---|---|---|---|
| Au-C | 1.00(20) | Au-$SiO_2$ | 1.3(3) |
| Ag-C | 0.41(30) | Au-$Al_2O_3$ | 1.1(3) |
| Pd-C | 1.17(30) | Au-sapphire[a] | 1.1 |
| Pt-C | 0.75(30) | Pd-$SiO_2$[b] | 1.6 |
| Cu-C[c] | 0.6 | Pt-$SrTiO_3$(100)[d] | 0.3 |
| Ni-C[c] | 0.6 | | |

[a]Reference 4.
[b]Reference 6.
[c]Reference 7.
[d]Reference 10.

ing energy. Such an effect is clearly impossible for an isolated atom, and thus a shift to lower $E_B$ is expected in the transition from atom to bulk metal. For supported metal clusters, this relaxation shift will depend on the relative abilities of the substrate and the bulk metal to shield the final-state hole. If the substrate is significantly less effective in this regard, then shifts of the type shown in Table I can easily result.

Binding-energy shifts are not the only effect to be expected from changes in relaxation. Linewidth is also critically dependent upon relaxation and should increase with decreasing screening.[29,30] Ascarelli and co-workers have proposed a theoretical model in which they were able to account for the line broadening of about 1 eV observed for small Au clusters supported on Teflon.[31] A similar broadening is observed in all XPS measurements of supported clusters.

Finally, Bahl and co-workers have used both XPS and AES to study Pt clusters on single-crystal strontium titanate ($SrTiO_3$).[10] In the simplest approximation, the change in relaxation energy can be derived from the combination of XPS binding energy $E_B$ and Auger kinetic energy $K$. These quantities define the Auger parameter[32] $\alpha = K + E_B$. The difference in the Auger parameters for a given element in two different environments is approximately twice the difference in relaxation energies,

$$\Delta\alpha \cong 2\Delta R \ . \tag{1}$$

A change in relaxation energy of 0.8 eV was calculated for low-coverage Pt relative to the bulk metal by using this method.[10]

Variations in the commonly measured parameters of linewidth, binding energy, and Auger kinetic energy all appear to be satisfactorily accounted for by the relaxation model. The next section examines the electronic structure model and attempts to account for experimental results in terms of initial-state electronic properties.

### B. Electronic structure model

In considering the transition from a free atom to the bulk metal, we concluded that fairly large changes in relaxation energy would necessarily take place. However, changes in the initial-state electronic structure are just as inevitable. As pointed out previously,[19] free atoms have integral configurations but bulk metals in general, and $d$-band metals in particular, do not. Contrary to the statements of Ref. 6, even the noble metals have nonintegral configurations. A full $d$ band is not equivalent to a $d^{10}$ configuration. Hybridization with empty states above the Fermi level reduces the true $d$-electron count.[26,27,33] This has been shown experimentally by x-ray absorption and electron energy-loss[34] studies and in numerous theoretical band calculations.[26,33–35] The repulsive Coulomb interaction between core and valence electrons will cause the core-electron binding energies to be very sensitive to the valence-electron configuration. Since valence $s$ and $p$ electrons of transition and noble metals are much more diffuse than the $d$ electrons, the core levels are expected to shift towards lower binding energy with increasing $d$-electron count. A similar but somewhat smaller shift is expected for the centroid $\epsilon_d$ of the valence $d$ bands themselves.[26] This effect can be very large, as shown by the 5.5-eV core-level shift calculated by Watson and Perlman for the $3d^8 4s^2 \rightarrow 3d^9 4s^1$ configuration change that occurs between atomic and bulk metallic nickel.[27] More modest values of about 1 eV are shown in Table I for the $E_B$ shift in supported clusters. In the presence of a support, not only can the final state be screened, but the initial state of the atoms need not be integral as in the free atom. As a result, the

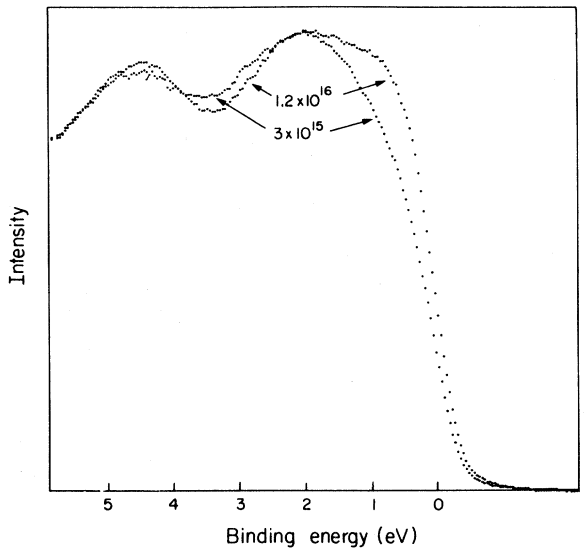


FIG. 1. Valence-band spectra of Pt clusters at two coverages. Note increase in intensity at the top of the $d$ band with increasing coverage. Average particle size for $3\times10^{15}$ atoms/cm$^2$ is about 18 Å; the particles are severely coalesced at $1.2\times10^{16}$ atoms/cm$^2$.

shifts are reduced relative to those of the simplified free-atom model.

The rest of this section presents data that support this configuration-change interpretation. I will also show how the data presented in the preceding section can be understood without invoking a large size dependence to the final-state relaxation processes.

The simplest experimental results that show an increase in $d$-orbital occupation with size are shown in Fig. 1, where the XPS valence-band spectra of platinum at two different coverages are compared.[5] An increased intensity at the topmost part of the band is observed for the highest coverage. Although this effect is largest for Pt clusters, it is also present in the other group-VIII metals we have studied (Pd, Rh, and Ir). The increased intensity is simply interpreted as an increase in the number of $d$ electrons present, the $5d$ ionization cross section being almost two orders of magnitude larger than the $6s$.[36] Other possibilities, such as enhancement of the $5d$ cross section itself, seem unlikely in view of the almost unaltered band shape above $\sim2$ eV binding energy. The dominant spectra changes are restricted to energies near the Fermi level, where differences in orbital occupation should be most noticeable.

If constant orbital ionization cross sections are assumed, the XPS results are a direct measure of the $d$-orbital occupation, the intensity being proportional to the number of electrons available for ionization. If the number of occupied $d$ orbitals is dependent on cluster size, it follows that the number of $d$ holes or vacancies is also size dependent in a complementary fashion. The number of $d$-orbital vacancies, or more properly stated, the amount of $d$ character in the vacancies near the Fermi level, can be measured directly by x-ray absorption spectroscopy (XAS). In x-ray absorption from a core $2p$ level ($L_{2,3}$ absorption), dipole selection rules restrict the final state to either an $s$ ($l=0$) or a $d$ ($l=2$) orbital. Calculations and experiments have shown that the $\Delta l=+1$ $d$ channel is strongly dominant to the point where the $p\rightarrow s$ transition need not be considered.[24] The intensity of absorption is then primarily dependent on the $p\rightarrow d$ transition matrix element and the number of $d$ final states available. When such $d$ vacancies are present the effect is manifested as a strong and sharp absorption maximum near the band edge and historically has been referred to as the "white line."[34,37] Although not quantitatively accurate, this technique has given impressive results in determining the relative density of $d$ vacancies in bulk metals and supported metal clusters.[38] I have applied this technique by measuring the $L_2$ ($2p_{1/2}\rightarrow 4d_{3/2}$) and $L_3$ ($2p_{3/2}\rightarrow 4d_{3/2,5/2}$) absorption for Pd at coverages ranging from $4.5\times10^{14}$ atoms cm$^{-2}$ to the bulk metal. At the lowest coverage most of the atoms are not atomically dispersed but are small clusters with an average diameter of $\sim8$ Å and containing $\sim9$ atoms. From the XPS criterion of increased binding energy and lower emission intensity near the Fermi level, these clusters are expected to be $d$-electron deficient and should show an enhanced "white line" adsorption. The measured absorption spectra for $L_2$ and $L_3$ edges are shown in Fig. 2, and as expected, the lower coverage spectra do show increased absorption in the "white line." The comparison of the spectra in Fig. 2 is somewhat subjective because of the difficulty in matching the spectra on the high-energy side, where the EXAFS oscillations occur. Nevertheless, the basic conclusion is independent of this uncertainty in that any reasonable matching of spectra shows an enhancement of "white line" intensity at low coverage.

Not only is the intensity of the XAS spectrum dependent on cluster size, but the energy of the transition also varies. A comparison of the XPS and XAS edge shifts is revealing for an assessment of the importance of extra-atomic relaxation. The XAS edge energy is that energy required to excite an electron from a core level to the first unoccupied orbital. The final state is then a highly excited state with a deep core hole and an extra valence electron. This is exactly the final state that would occur for the XPS measurement in the complete screening limit.[25] Therefore, the degree to which the XPS fi-

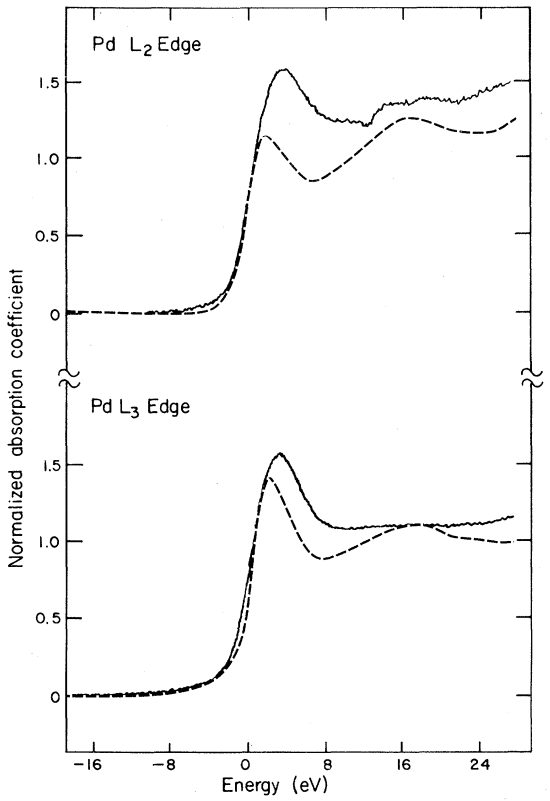


FIG. 2. $L_2$ and $L_3$ absorption edges of Pd at coverages of $4.8\times10^{14}$ atoms/cm$^2$ (——) and $1.35\times10^{17}$ atoms/cm$^2$ (— — —).

nal state is not completely screened can be measured by the degree to which the XPS and XAS shifts differ. These measurements have been made for two systems: Pd-C and Cu-C (Table II). The shifts are identical within experimental error. This strongly suggests that final-state extra-atomic relaxation effects are complete at the smallest cluster sizes and that the shifts in core-level binding energies are the result of changes in initial-state properties. This conclusion is also supported by the results given in Table I. If the screening were incomplete for the small clusters, large changes would be expected in the core-level shifts as the substrate is varied. The

TABLE II. Comparison between XPS and XAS shifts.

| | XPS (eV) | XAS (eV) |
|---|---|---|
| Pd-C | 1.15(20) | 0.3(3) |
| Cu-C | 0.7(2)[a] | 0.7(2)[b] |

[a]Reference 7.
[b]Reference 9.

binding-energy shift for Au varies by less than 20% in going from the conducting semimetal carbon to such good insulators as $SiO_2$ or $Al_2O_3$ (Table I). The relationship between substrate and binding-energy shift will be dealt with in greater detail in Sec. V.

If the changes in extra-atomic relaxation are relatively small, then one is faced with the problem of explaining the linewidth and Auger results referred to in the preceding section. The increased linewidth at low coverage can easily be explained as the result of a distribution of absorption sites for the small clusters. Electron microscopy studies have clearly shown that the absorption sites are not all equivalent and that the number of sites $n_s$ varies with both substrate and metal.[21–24] In Fig. 3 the observed increase in linewidth is plotted against the number of active absorption sites for Ag, Au, and Pd on several amorphous substrates. The Pd results are corrected for the many-body effects on the line shape, which produce strong asymmetries in the bulk metal.[40] The correlation between $n_s$ and the observed line broadening is considered excellent in view of the experimental uncertainties. Furthermore, we have measured the linewidth of Au absorbed at low temperatures on several different metallic substrates and have found broadening comparable to that observed on amorphous carbon. As would be expected for an inhomogeneous site broadening, these linewidths decrease significantly when the sample is warmed to room temperature, where the atoms are free to diffuse to more equivalent lower-energy positions. For example, the full width at half-maximum (FWHM) of Au on Cd decreases from 1.65 to 0.86 eV and that of Au on Pt from 2.0 to 1.2 eV on warming from 160 K to room temperature.

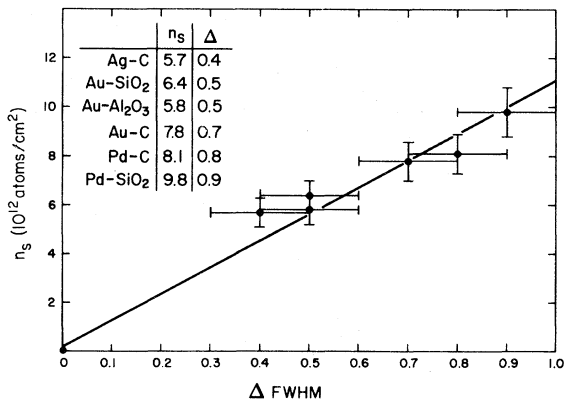


FIG. 3. Number of active sites $n_s$ vs the increase in linewidth relative to the bulk metal. $n_s$ values and uncertainties are from Ref. 39. Inset gives the values of $n_s\times10^{-12}$ atoms/cm$^2$ and ΔFWHM for the various atom-metal combinations.

Accounting for the large changes of extra-atomic relaxation calculated from XPS and AES shifts requires a detailed look at the approximations used in the analysis. To address this question we have measured the Auger spectra at low coverages for Ag, Au, Pd, and Pt on amorphous carbon supports. The results are shown in Table III along with those of Ni from Ref. 41. Based on the model used by Bahl and co-workers,[10] the calculated changes in relaxation energies can account for 30—100% of the measured XPS shift. However, the uncertainties of the measurements represent a significant fraction of the shifts. These large uncertainties are easily understood. In both XPS and AES measurements the energies of interest were determined relative to a calibrating substrate level. In this work $E_B$ was generally measured relative to the substrate C 1$s$ ($E_B = 284.6$ eV, FWHM$\cong$1.6 eV for the amorphous material), and the AES energies were relative to the Ar $LMM$ ($E_K = 212.0$ eV, FWHM$\cong$3.3 eV on derivative peak). Furthermore, the cluster lines themselves, particularly in AES, become quite broad at low coverage. The determination of shifts by the difference in energy of broad lines leads to the considerable uncertainties in Table III. These qualifications aside, the primary conclusion remains that extra-atomic relaxation appears to contribute significantly to the total energy shift. The problem in this analysis may lie in the oversimplification of the model. Thomas has shown that Eq. (1) results from only the first two terms in a Taylor-series expansion of the binding and Auger kinetic energies.[32] The higher-order terms generally lower the resulting relaxation energies. Taking these expansions to higher order, Thomas has shown that

$$\Delta R = \frac{\Delta\alpha}{2} + \frac{2}{3}\Delta\left[\left[\frac{dk}{dN}\right]\left[\frac{dq}{dN}\right]\right], \qquad (2)$$

where $dk/dN$ is a negative quantity representing the change in the size of the valence orbitals due to the loss of the core electron and $dq/dN$ represents the transfer of screening charge to the valence orbitals.

No data are available to quantitatively assess the effects of these higher-order terms in atom-to-metal transitions, but work has been done with simple molecular systems.[32] In such systems, not only do the higher-order corrections lower the resulting relaxation energies, but their effect is largest for molecules with the greatest number of polarizable ligands. Extension of this trend to metal clusters or bulk metals would suggest that the results in Table III overestimate the changes in extra-atomic relaxation.

Finally, I emphasize again that changes in the orbital occupations or configurations with cluster size are to be expected for all metals where the bands are hybridized near the Fermi level. This includes all of the transition and noble metals as well as many of the rare earths. In fact, for the rare-earth metal Sm, a change in configuration with particle size has been proven unambiguously.[19] Because of the large 3$d$ core-level shifts and distinctive 4$f$ multiplet structure, a change from the divalent ($4f^6$) configuration in the small cluster to the trivalent ($4f^5$) in the bulk could be clearly established. Furthermore, these clusters become "bulklike" over the same size range as reported here for the transition and noble metals. The only difference in establishing the configuration changes in rare earths relative to $d$-band metals is the small size of the 4$f$ orbitals of the rare earths as compared to the more diffuse valence $d$ orbitals of the transition and noble metals. This contracted size leads to enhanced core-level shifts and resolvable 4$f$ multiplet structure. Samarium differs from the $d$-band metals in the degree to which configuration changes affect the measurable spectral properties, but not in the basic physical processes that take place.

The next section continues to address this question of changes in configuration with cluster size. Close similarity will be shown between metal clusters and metal alloys, and a thermodynamic model will be applied for calculating core-level shifts. Both of these exercises will further substantiate the conclusion of this section—that electronic configu-

TABLE III. Relaxation shifts in metal clusters.

| Shift (eV) | Ag[a] | Au[b] | Pd[a] | Pt[a] | Ni[c] |
|---|---|---|---|---|---|
| XPS core-level shift | 0.41(30) | 1.00(20) | 1.17(30) | 0.75(30) | 0.9(1) |
| Auger level shift | 1.2(3) | 1.68(30) | 2.18(30) | 1.96(30) | 0.9(1) |
| $\Delta = 2\Delta R$ | 0.8(4) | 0.68(36) | 1.01(42) | 1.21(42) | 0(1) |
| $\Delta R$ | 0.4(2) | 0.34(18) | 0.50(21) | 0.61(21) | 0(1) |

[a]Electron-excited Auger.
[b]Photon, $h\nu = 1486.6$ eV, excited Auger.
[c]Reference 41.

ration changes and not relaxation changes are primarily responsible for the measured spectral shifts.

## IV. CLUSTERS AND ALLOYS

The similarity between supported metal clusters and alloys was first pointed out by Roulet and coworkers in a study of Au clusters on alkali halide supports.[11] This work established a correlation between the Au $5d$-band width and the average coordination number $\bar{n}$. This section will give photoemission results from clusters and alloys and establish that $\bar{n}$ is indeed a valid indicator of the electronic structure. After the relationship between clusters and alloys is established, the extensive results available for alloys will be applied to help understand the electronic structure of the metal clusters. Most of the experimental results will deal with Au clusters and alloys. The limitation to a single metal is strictly to make the experimental task more tractable. Gold was chosen as the principal metal because of the many available data and the resulting detailed understanding of the alloys.[26,27,33,42–46]

### A. Similarity between clusters and alloys

The XPS spectra of Au-Cd alloys, reported by Shevchik,[43] are almost identical with those of Au clusters on carbon supports.[16] The changes in the valence $5d$ binding energies with cluster and alloy concentration parallel each other exactly. The splitting goes from 1.4 eV at low alloy concentrations and cluster size to about 3.0 eV in the bulk metal.[47] In both cases the increased peak separation is due to an asymmetric shift of the two $d$ components. The high-binding-energy component remains almost stationary, but the low-binding-energy peak moves towards the Fermi level with increasing particle size or gold concentration. A comparison of the core-level shifts further emphasizes the similarity of alloys and clusters. The gold $4f$ lines in both systems shift by 1.0 eV to higher binding energy as the size or the concentration decreases. In fact, the only significant difference between the alloy and cluster spectra is the expected linewidth increase observed in clusters at low coverages.

To explain the concentration dependence of the $5d$ alloy spectra, Shevchik proposed a simple molecular-orbital model that included the effects of overlap on adjacent atoms.[48] In this treatment the molecular-orbital energies are given by

$$E_{b,a}=\frac{\pm VS(n)}{1\pm S(n)} \ . \tag{3}$$

The $+$ and $-$ are associated with the bonding and antibonding orbitals, respectively, $V$ represents the interaction between the Au $d$ orbitals on adjacent sites, and $S(n)$ is an overlap integral, which is dependent on the number of like nearest neighbors $n$. The observed asymmetry in the $5d$ splitting is correctly accounted for by this model. The denominator in Eq. (3) causes the low-binding-energy, antibonding orbitals to shift much more than the bonding orbitals. In the allowed range of $S$ (0 to 1), $E_b$ varies from 0 to $V/2$ and $E_a$ goes from 0 to $-\infty$. The qualitative conclusions of this simple model have been verified by self-consistent band-structure calculations on a number of intermetallic compounds.[49]

This model emphasizes the importance of $n$, the number of like nearest neighbors, in determining electronic structure. The prominent role of like-neighbor interactions in alloys was first pointed out by Friedel[50] and has been emphasized in the photoemission studies by Nicholson and co-workers.[44] In view of the well-established importance of this parameter in alloys and the qualitative similarity of alloys and clusters in photoemission, it seems reasonable that $n$ may also be of primary importance in determining the electronic structure of clusters. Therefore, if the average coordination number for like atoms $\bar{n}$ can be determined for alloys and clusters, their experimental results might be compared more quantitatively. In other words, photoemission results from an alloy could be compared with those of clusters with the same average coordination. The average coordination of like atoms in a random alloy is easily determined. The number of identical neighbors is given by a binomial distribution with the mean coordination number $\bar{n}$ being the mean of the distribution,

$$\bar{n}=NP \ . \tag{4}$$

Here $N$ is the total coordination number, equal to 12 for a fcc structure, and $P$ is the fractional concentration of the atoms of interest.

The value of $\bar{n}$ for Au clusters on carbon is shown in Fig. 4. The mean cluster size for a given metal coverage is determined from the work of Preuss and Hamilton.[39] The circles are calculated for discrete clusters using highly symmetrical geometries.[51] At the higher coverages, $\bar{n}$ was calculated from the surface-to-volume ratio assuming surface and bulk coordination numbers of 8 and 12. These values are represented by triangles in Fig. 4. Although Fig. 4 extends to a coverage of about $4\times10^{15}$ atoms/cm$^2$, the clusters have in fact begun to coalesce at around $1\times10^{15}$ atoms/cm$^2$. This problem, however, does not become severe until about $6\times10^{15}$ atoms/cm$^2$, at which point $\bar{n}$ can no longer be determined accurately.[39] This limitation is only minor, because most of the binding-energy shifts in both core and valence

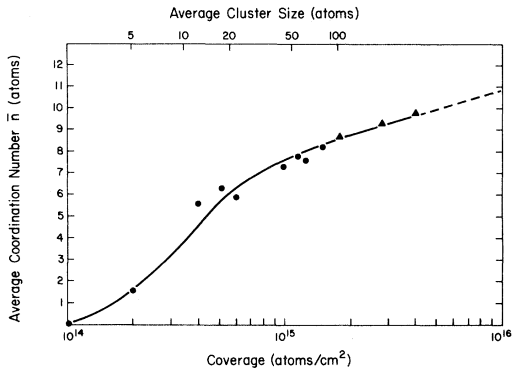


FIG. 4. Average coordination number $\bar{n}$ vs metal coverage for gold deposited on carbon. Average number of atoms per cluster is given on the upper axis. Circles represent values calculated from discrete cluster geometries of high symmetry. Triangles are calculated from surface-to-volume ratios assuming surface and bulk coordination of 8 and 12, respectively. Plot is based on data in Ref. 39.

levels occur below these limiting coverages.

Having determined the relationships between coordination number, alloy concentration, and metal coverage, we can now directly compare alloy and cluster spectra. Figure 5 shows the variation in gold $5d$ splitting as a function of $\bar{n}$ for gold clusters and alloys. The closed circles represent cluster results, and the open circles are the XPS results of Shevchik for Au-Cd alloys.[43] The agreement between these two sets of data is extremely good, especially in view of the experimental uncertainties, $\geq 0.1$ eV, and the fact that no adjustable parameters are involved. A similar comparison of the core-level shifts in alloys and clusters is complicated by the lack of consistent experimental data. However, where either the core- or valence-level shifts of Au alloys were studied in

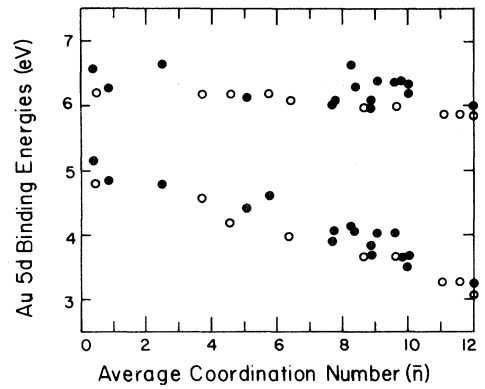


FIG. 5. Au $5d$ binding energies vs the average coordination number $\bar{n}$ for gold clusters on carbon supports (●) and for gold-cadmium alloys (○), Ref. 43.

detail, the shift varied almost linearly with Au concentration and hence $\bar{n}$.[42–44,52] Such a quasilinear relationship has also been assumed in some theoretical treatments of alloys.[53] These results confirm the linear dependence of Au binding energies on concentration and $\bar{n}$ for the type of alloys considered here. Figure 6 shows that the core-level binding energies of clusters also depend linearly on $\bar{n}$. Here the core-level shifts of Pd, Pt, and Au clusters are plotted against $\bar{n}$. The solid lines represent linear least-squares fits and give 0.96, 0.93, and 0.94 for the coefficients of determination in Pd, Pt, and Au, respectively. The largest deviation from the linear dependence is at high values of $\bar{n}$, which correspond to coverages where coalescence effects cause the calculated $\bar{n}$ values to be somewhat low.

### B. Gold supported on other metals

To further establish the validity of comparing carbon-supported clusters and alloys, we have examined gold supported on a number of metal substrates and on the insulators silica and alumina. A secondary object of these experiments was to gain some insight as to why noble and group-VIII metals shift to higher $E_B$ in small clusters and to lower $E_B$ on the surface of the bulk metal.[54,55]

Gold $4f_{7/2}$ binding-energy shifts are summarized in Table IV. Because electron microscopy to obtain a particle size distribution cannot be done on metallic supports, we have restricted our measurements to low coverages at low temperature, where the atoms are most likely to be atomically dispersed. However, the nucleation process on metallic substrates has not been characterized, and it is possible that the atoms do not exist entirely as isolated species. As a result, the values listed in Table IV should be considered only as lower limits for the true atom-to-bulk shifts. On alumina and silica the size distributions have been determined,[39] and the $4f_{7/2}$ binding energies have been measured over the entire range from isolated atoms to bulk metal. These results are shown in Fig. 7 along with the previously reported carbon data.

The qualitative variations in binding energy shown in Table IV range from $+1.2$ to $-0.66$ eV and can be understood quite simply from Eq. (3). In the preceding section, when carbon or cadmium supports were considered, the parameters $V$ and $S(n)$ were defined in terms of interactions only with neighbors of the same type. In actuality, these parameters are determined by interactions with all neighbors, regardless of type. If the host is a metal such as Cd, there is only a broad, diffuse $s$-$p$ conduction band in the binding-energy region of the Au $5d$'s. The interactions between the $5d$'s and the

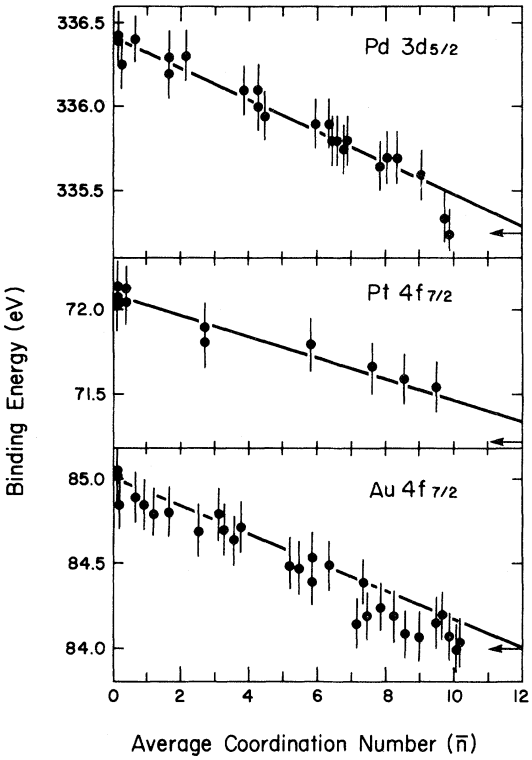


FIG. 6. Core-level binding-energy shifts for Pd, Pt, and Au on carbon supports as a function of average coordination number $\bar{n}$. Error bars are rough estimates of the experimental uncertainties. Solid lines are linear least-squares fits to the experimental data.

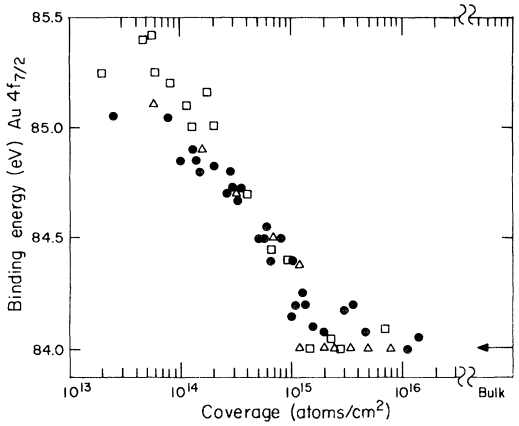


FIG. 7. Au $4f_{7/2}$ binding energy vs metal coverage for Au supported on carbon (●), $SiO_2$ (□), and $Al_2O_3$ (△) supports.

host conduction band are very weak compared to the $d$-$d$ interaction between adjacent Au atoms. Hence with hosts such as Cd, Zn, or C the interaction energy and overlap are, to a good approximation, determined solely by the number of like neighbors. However, when the host or substrate has occupied "quasiatomic" $p$ or $d$ levels in the energy region of the Au $5d$'s, the situation is quite different and interactions with these states must be considered.[57] This is illustrated by the $E_B$ shifts that occur when Au is supported on the $4d^{10}5s^25p^n$ ($n=0$–4) elements in the series in Table IV from Cd to Te. The separation between the Au $5d_{3/2}$ level and the $4d$ levels ranges from about 4 eV in Cd to almost 35 eV in Te. Since no substrate $4d$–Au $5d$ interaction is apparent in Cd, we assume that it is negligible throughout the series from Cd to Te. The dominant interaction for Au on these substrates appears to be between the uppermost $5d$ level of gold, the $5d_{5/2}$ level of the free atom, and the $5p$ levels of the support. Figure 8 shows the bottom of the substrate $5p$ band[58,59] along with that of the Au $5d$'s.[60] The $p$-$d$ interaction will be repulsive and will increase as the energy separation decreases. As a result, when the substrate $p$ levels are above the Au $5d$'s, the interaction will cause the gold levels to shift to lower energy or higher binding energy. The resulting change in atomic potential will cause the core levels to shift in a parallel manner.[26,42] These conclusions agree

TABLE IV. Au $4f_{7/2}$ core-level binding-energy shifts on various substrates.

| Substrate | Shift (eV) | Substrate | Shift (eV) |
|---|---|---|---|
| C | 1.0(1) | Pd | −0.66(10) |
| Cd | 0.73(10) | Pt | −0.30(10) |
| In | 0.98(10) | Ni[a] | −0.23(5) |
| Sn | 1.06(10) | Au[b] | −0.40(1) |
| Sb | 0.20(10) | Au[c](100)-(5×20) | −0.28(1) |
| Te | −0.46(10) | Au[c](100)-(1×1) | −0.38(1) |
| $SiO_2$ | 1.2(1) | Au[c](110) | −0.35(1) |
| $Al_2O_3$ | 1.1(1) | Au[c](111) | −0.35(1) |

[a]Reference 56.
[b]Reference 55.
[c]Reference 54.

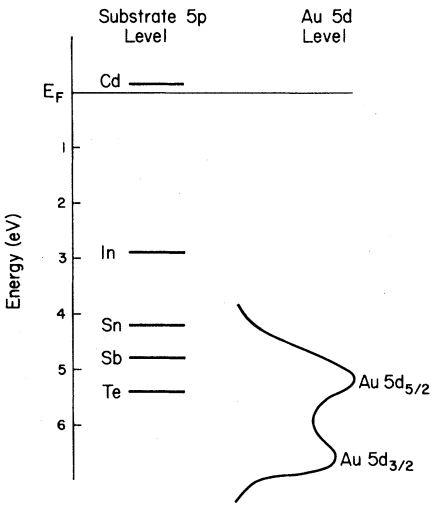


FIG. 8. Left-hand column shows the position of the bottom of the metal $p$ band in Cd, In, Sn, Sb, and Te. These values were determined from the photoemission results of Ref. 58 and the band-structure calculation of Ref. 59. Right-hand column represents the position of the Au $5d$ levels as measured for Au atomically dispersed on a carbon substrate, Ref. 60.

with the results in Table IV and Fig. 9 that show an increase in binding-energy shift from Cd to Sn. For Sb or Te, the substrate $p$ levels overlap the Au $5d$'s, and the shift decreases (Sb), then actually changes sign (Te), as the $p$ level drops below the highest $5d$ level. Similar effects are seen in Au alloys[42,46] or when Au is deposited onto metals whose $d$ bands overlap those of gold.[56] The binding-energy shifts are always to lower values when the energies of the interacting states overlap significantly. Under these conditions, the Au atoms are intimately involved in

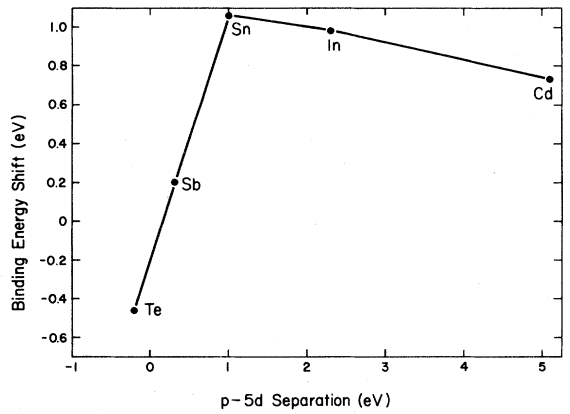


FIG. 9. Measured Au $4f_{7/2}$ binding-energy shifts on Cd, In, Sn, Sb, and Te vs the separation between the bottom of the substrate $p$ levels and the top of the Au $5d$ band.

the band structures of the host or substrate metal, and the simplistic model presented above may be insufficient to describe the interactions. However, the decrease in binding energy that is observed when the host or substrate $d$ bands fall below the Au $5d$ levels is at least consistent with the expectation of Eq. (3).

A special case of overlapping levels occurs at the surface of pure metals. Here, even in the absence of reconstruction, the surface atoms differ from the bulk at least by virtue of their lower coordination. However, the energy levels of these surface atoms will overlap the energy bands of the bulk metal. For $d$-band metals with more than five $d$ electrons, the core-level shifts are always to lower $E_B$.[54,55] These shifts have been investigated by many groups and are fairly well understood.[54,55,61,62] Owing to the lower coordination at the surface, the "surface band" is narrower but the Fermi level must be equalized from bulk to surface. This requires (for a more than half-filled $d$ band) the surface band to shift upward to lower binding energy, a shift which will be reflected in the core $E_B$. This argument should hold for any surface atom with strongly interacting orbitals.

The difference in core-level shifts found at the surface of $d$-band metals and those of clusters is now understandable. On substrates such as carbon, cadmium, or zinc, there are no localized substrate levels in the energy range of the Au $5d$'s. The cluster binding energies are then determined by the $5d$-$5d$ interactions between adjacent Au atoms and will increase with decreasing coordination or cluster size. If the substrate itself has states that can interact strongly with the cluster levels, these interactions will further modify the binding energies. Normally the substrate levels are above the cluster $d$ orbitals, and the repulsive interaction results in a shift to higher binding energy. If the two interacting orbitals overlap in energy, the cluster orbitals must be considered as part of the substrate band structure and the binding energy will normally be lower than that of the bulk metal.

### C. Electronic structure of clusters and alloys

Much of the preceding has been devoted to establishing the validity of cluster-alloy comparisons. A principal motivation for this is that we can now apply the vast knowledge of electronic structure in alloys to the study of clusters. This is one of the primary reasons for the emphasis on gold in our cluster studies. Gold alloys have been studied extensively by Mössbauer and photoemission spectroscopy. Combining those techniques, Watson and coworkers have studied the charge-transfer effects of alloying.[26,27,42] Since Mössbauer isomer shifts are

TABLE V. Charge variation in Au alloys and intermetallics.

| Alloy | $\Delta n_c$ | $\Delta n_d$ | $\delta$ | $\Delta n_c/\Delta n_d$ |
|---|---|---|---|---|
| AuTe[a] | 0.19 | −0.11 | 0.08 | −1.7 |
| AuSn[a] | 0.33 | −0.20 | 0.13 | −1.7 |
| AuIn[a] | 0.40 | −0.20 | 0.20 | −2.0 |
| AuCd[b] | 0.28 | −0.19 | 0.09 | −1.5 |
| AuZn[b] | 0.29 | −0.22 | 0.07 | −1.3 |
| AuCu[b] | 0.36 | −0.24 | 0.12 | −1.5 |
| $AuSb_2$[a] | 0.27 | −0.16 | 0.11 | −1.7 |
| $AuGa_2$[a] | 0.50 | −0.29 | 0.19 | −1.7 |

[a]Reference 47.
[b]Reference 26.

sensitive to the *s*-electron density and XPS core-level shifts are most affected by the 5*d* density, the combination of these techniques allows complete determination of the valence-electron charge distribution. The changes upon dilute alloy formation of the 6*s*-electron count $\Delta n_c$ and the 5*d*-electron count $\Delta n_d$ can both be determined. The results are given in Table V, along with the net interatomic charge transfer $\sigma$ and the ratios of $\Delta n_c/\Delta n_d$. In all cases the *d*-electron count is depleted in comparison to the bulk metal, and the number of 6*s* electrons increases. Owing to this compensation, the net charge transfer is small, normally less than 0.2 electron/atom, and has little direct effect on measured $E_B$ shifts. This result has been borne out by self-consistent band-structure calculations for a series of intermetallic compounds.[49] Furthermore, this study strongly supports our conclusion about the electronic structure of small clusters. Specifically, small clusters are *d*-electron deficient in comparison to the bulk metal, but very little net charge transfer to the substrate occurs.[5] The clusters maintain near neutrality and essentially rehybridize as a result of interaction with the substrate. The variation in 6*s* and 5*d* electron count can completely account for the core-level shifts in clusters on weak supports. Since the Coulomb repulsion between a core and a 5*d* electron is greater than between a core and the more diffuse 6*s* electron,[63] the binding energy will be increased in the *d*-deficient clusters. A similar effect will be felt by the valence electrons themselves, but will be smaller because of the diminished value of the 5*d*-5*d*(6*s*) repulsion compared to that of the core-5*d*(6*s*).

## V. THE THERMODYNAMIC MODEL

A simple thermodynamic model of core-level binding-energy shifts was developed recently by Johansson and Mårtensson.[25] Several papers have discussed their model and its applications in considerable detail[46,53,56,62,64]; such a discussion will not be repeated here. For our purpose the important virtue of this model is its ability to accurately predict binding-energy shifts resulting from changes in an atom's environment, e.g., gas to solid, bulk to surface, or pure metal to alloy. This model avoids the common difficulties in reference levels by inherently referencing solid-state $E_B$ to the sample Fermi level. Furthermore, the shifts can be calculated from thermodynamic quantities determined independently of any photoemission measurements.

In this section, the Johansson and Mårtensson model will be used to calculate the binding energy, relative to the pure metal, of atom *A* on support *B*. The problem can be conveniently divided into two parts. First we will consider the shift produced by forming the dilute bulk alloy of *A* in *B* and then the effects of bringing atom *A* to the surface of host *B*. This exercise will further establish the similarity between alloys and clusters. Furthermore, the model allows a clear quantitative distinction between initial- and final-state contributions to the binding-energy shifts and hence an independent test of the initial-state model presented in Sec. III B.

### A. Binding-energy calculations

The binding-energy shift that results when an atom *A* is removed from the pure metal and dissolved in host *B* can be written[46]

$$\Delta E^b_{\text{calc}} = E(A;B) + E(A+1;A) - E(A+1;B), \tag{5}$$

where the superscript *b* refers to the atom being dissolved in the bulk. Terms of the form $E(A;B)$ represent the energy of solution of atom *A* in host *B*, and $A+1$ refers to the element with atomic number one greater than that of *A*. The first term $E(A;B)$ represents the change in the initial-state energy of atom *A* upon solution in *B* [$E(A;A)$ being zero by definition]. The remaining two terms, $E(A+1;A)$ and $E(A+1;B)$, represent the difference in final-state energies in hosts *A* and *B*. In this model the final state of atom *A* is assumed to be completely screened and is approximated by the energy appropriate to the $A+1$ atom. The solution energy terms on the right side of Eq. (5) can be determined from thermochemical measurements.[65] However, such data are not available for many of the systems of interest. We have, therefore, followed the common practice of calculating the heats of solution using the semiempirical scheme of Miedema.[66] Following closely the presentation in Ref. 46, the solution energy at low concentrations $E(A;B)$ can be expressed as

TABLE VI. Calculated solution energies and core-level binding-energy shifts for dilute alloys; also given are the experimental shift and the difference Δ.

| *A-B* | $E(A;B)$ | $E(A+1;A)$ | $E(A+1;B)$ | $\Delta E^{\text{bulk}}_{\text{calc}}$ | $\Delta E^{\text{surf}}_{\text{expt}}$ | Δ |
|---|---|---|---|---|---|---|
| Ni-C | 2.15 | −0.22 | 1.07 | 0.86 | 0.6 | 0.26 |
| Pd-C | 1.98 | 0.23 | 0.77 | 1.44 | 1.10 | 0.30 |
| Pt-C | 2.23 | −0.16 | 0.67 | 1.40 | 0.90 | 0.50 |
| Ag-C | 0.77 | 0.14 | 0.45 | 0.46 | 0.41 | 0.05 |
| Cu-C | 1.07 | 0.31 | 0.89 | 0.49 | 0.6 | −0.11 |
| Au-C | 0.67 | 0.28 | −0.09 | 1.04 | 1.00 | 0.04 |
| Au-Zn | 0.90 | 0.28 | −0.05 | 1.23 | 1.20 | 0.03 |
| Au-Cd | 0.57 | 0.28 | 0.02 | 0.83 | 0.73 | 0.10 |
| Au-In | 0.58 | 0.28 | 0.04 | 0.82 | 0.98 | −0.16 |
| Au-Sn | 0.55 | 0.28 | 0.00 | 0.83 | 1.06 | −0.23 |
| Au-Sb | 0.32 | 0.28 | 0.03 | 0.57 | 0.20 | 0.37 |
| Au-Pd | 0.14 | 0.28 | 1.64 | −1.22 | −0.66 | −0.56 |
| Au-Pt | −0.16 | 0.28 | 0.72 | −0.60 | −0.30 | −0.30 |
| Au-Ni | −0.31 | 0.28 | −0.04 | −0.02 | −0.23 | 0.21 |
| Au-Te[a] | −0.34 | 0.28 | 0.13 | −0.20 | −0.46 | 0.26 |
| Au-Al | 1.15 | 0.28 | −0.21 | 1.64 | 1.7 | −0.06 |
| Ag-Al | 0.31 | 0.14 | −0.17 | 0.62 | 0.7 | −0.08 |
| Co-Al | 1.12 | 0.01 | 1.27 | −0.14 | 0.0 | −0.14 |
| Ni-Al | 1.27 | −0.22 | 0.44 | 0.61 | 0.5 | 0.11 |

[a]Parameters for Eq. (7) determined by extrapolation of published values for the $4d\,5s\,5p$ metals (Ref. 66).

$$E(A;B)=\frac{2V_A^{2/3}(1+a\Delta\phi^*)P}{\eta_{\text{WS}}(A)^{-1/3}+\eta_{\text{WS}}(B)^{-1/3}} \times(|\Delta\phi^*|^2+R-9.4|\Delta\eta_{\text{WS}}^{1/3}|^2)\,, \quad (6)$$

$$\Delta\phi^*=\phi_A^*-\phi_B^*,\quad \Delta\eta_{\text{WS}}^{1/3}=\eta_{\text{WS}}(A)^{1/3}-\eta_{\text{WS}}(B)^{1/3},$$

$$P=0.128,\quad a=0.09.$$

The parameters $V$, $\phi^*$, $\eta_{\text{WS}}$, and $R$ are empirically determined, but in Miedema's formalism each has a specific physical meaning.[69] The first three quantities are characteristic of the pure metals, $V$ representing the atomic volume, $\phi^*$ a slightly modified work function or chemical potential, and $\eta_{\text{WS}}$ the electron density at the boundary of the Wigner-Seitz unit cell. The parameter $R$ represents a *p-d* hybridization energy, which is nonzero only when one of the alloy constituents is a nontransition, *p*-electron metal. From the extensive tabulations of these parameters,[66] fairly accurate heats of solution can be determined for calculating binding-energy shifts in Eq. (5).

The results of such calculations are given in Table VI,[69] which lists the individual contributions to the $E_B$ shift [Eq. (5)] as well as the total calculated and experimental values and their differences. The close agreement between the $E_B$ shift calculated for the dilute alloy and that measured for the surface species shows that the surface-to-bulk shift in $E_B$ must in general be small. This has been verified directly for the 14 *A*/*B* combinations in Table VII.

TABLE VII. Experimental values for binding-energy shifts of metal *A* in metal *B* and metal *A* on metal *B*.

| *A-B* | ΔE (eV) bulk alloy | ΔE (eV) *A* on *B* | Δ (eV)[a] |
|---|---|---|---|
| Au-Zn | 1.09(5)[b] | 1.20(10) | 0.11 |
| Au-Cd | 1.00[c] | 0.73(10) | −0.27 |
| Au-In | 0.86(5)[b] | 0.98(10) | 0.12 |
| Au-Sn | 1.35(5)[b] | 1.06(10) | −0.29 |
| Au-Sb | 0.22(2)[b] | 0.20(10) | −0.02 |
| Au-Pd | −0.40(5)[b] | −0.66(10) | −0.26 |
| Au-Pt | −0.30(5)[b] | −0.30(10) | 0 |
| Au-Ni | 0.10(5)[b] | −0.23(5)[d] | −0.33 |
| Au-Al | 1.35(5)[b] | 1.5[e] | 0.35 |
| | 1.95(5)[b] | 1.7(1)[f] | −0.25 |
| Ni-C | 0.9[g] | 0.6(1)[h] | −0.03 |
| Ni-Al | 0.40(10)[i] | 0.5(1)[f] | 0.1 |
| Pt-C | 1.0(1)[j] | 0.75(10) | −0.25 |
| Co-Al | 0.00(10)[i] | 0.0(1)[f] | 0 |
| Au-$SiO_2$ | 1.1[f] | 1.3(3) | 0.2 |

[a]$\Delta=\Delta E(A \text{ on } B)-\Delta E$ (bulk alloy).
[b]Reference 42.
[c]Reference 43.
[d]Reference 56.
[e]Reference 4.
[f]Reference 67.
[g]Reference 41.
[h]Reference 7.
[i]Reference 46.
[j]Reference 68.

TABLE VIII. Calculated values of the initial- and final-state contributions to the binding-energy shifts of atom $A$ on support $B$.

| $A$-$B$ | Initial-state shift $\Delta E_i$ (eV) | Final-state shift $\Delta E_f$ (eV) | $\Delta E_i/\Delta E_f$ |
|---|---|---|---|
| Ni-C | 2.15 | −1.29 | −1.7 |
| Pd-C | 1.98 | −0.54 | −3.6 |
| Pt-C | 2.23 | −0.83 | −2.7 |
| Cu-C | 1.07 | −0.58 | −1.8 |
| Ag-C | 0.77 | −0.31 | −2.5 |
| Au-C | 0.67 | 0.37 | 1.8 |
| Au-Zn | 0.90 | 0.33 | 2.7 |
| Au-Cd | 0.57 | 0.26 | 2.2 |
| Au-In | 0.58 | 0.24 | 2.4 |
| Au-Sn | 0.55 | 0.28 | 2.0 |
| Au-Sb | 0.32 | 0.25 | 1.3 |
| Au-Pd | 0.14 | −1.36 | −0.1 |
| Au-Pt | −0.16 | −0.44 | 0.4 |
| Au-Ni | −0.31 | 0.32 | −1.0 |
| Au-Te | −0.34 | 0.15 | −2.3 |
| Au-Al | 1.15 | 0.49 | 2.4 |
| Ag-Al | 0.31 | 0.31 | 1.0 |
| Co-Al | 1.12 | 1.26 | 0.9 |
| Ni-Al | 1.27 | −0.66 | −1.9 |

Here the $E_B$ values of atom $A$ in the bulk of $B$ are compared with those of $A$ supported on the surface of $B$. The rms surface-to-bulk shift is only about 0.2 eV, with the largest value being −0.33 eV. Considering that the bulk and surface measurements were made by different investigators, the agreement is remarkable. The relatively minor effect on $E_B$ due to the surface allows us to look at the shifts primarily in terms of alloy formation. In particular, the question of initial- versus final-state effects can be addressed from this perspective. The first term in Eq. (5) gives directly the change in initial-state energy, and the remaining two represent the difference in final-state energies of the alloy and the pure metal. Table VIII lists these initial- and final-state shifts along with their ratios $\Delta E_i/\Delta E_f$. Where the $A$-$B$ interaction is expected to be weak (see Sec. IV), the initial-state effects are dominant. Conversely, in systems with strong $A$-$B$ interactions, the initial-state shifts are smaller and the final-state effects assume a greater relative importance. The dominant role of the initial state for substrates such as carbon agrees with the conclusion of Secs. III and IV and with those of our earlier studies.[5] It is also worth noting the fallacy of the intuitive concept[7] that relaxation energies are larger for bulk metals than for the metal atom on a support such as carbon. The results in Table VIII show that for Ni, Pd, Pt, Cu, and Ag on carbon the final-state relaxation energies are actually less in the bulk metal than for the carbon-supported atom. With the excellent agreement that this model gives for the total $E_B$ shifts, this conclusion seems valid.

## VI. CONCLUSIONS

Both experiment and theory have shown that the binding-energy shifts observed in small metal clusters on a support such as carbon are due primarily to initial-state effects. The photoemission spectra of clusters are quantitatively similar to those of bulk alloys. In fact, the binding-energy shifts observed in clusters can be accurately calculated by use of a simple thermodynamic model for shifts in alloy systems. The shifts can be to either higher or lower $E_B$, depending on the nature of the supporting substrate. When the substrate has localized $p$ or $d$ orbitals with binding energies that overlap those of the cluster $d$ orbitals, the shifts are generally to lower $E_B$. For less interactive substrates such as carbon, the metal-support interaction is weak and the shifts are to higher $E_B$ for the clusters relative to the bulk metal. For weakly interacting substrates, the variation in core-level binding energy and the valence $d$-

band splitting are linear functions of average coordination number $\bar{n}$. The $E_B$ shifts are caused by an increase in the $d$-electron count with increasing size. The variation in $d$-electron count is thought to result from $(s,p)-d$ rehybridization or intra-atomic charge transfer. The total net substrate-metal charge transfer is thought to be fairly small, about $0.1e^-$.

ACKNOWLEDGMENTS

I am indebted to W. F. Egelhoff, Jr., G. Apai, D. R. Preuss, P. H. Citrin, and G. K. Wertheim for making results available before publication. Many helpful discussions with R. E. Watson, J. F. Hamilton, Jr., S.-T. Lee, T. D. Thomas, R. C. Baetzold, and E. M. Shustorovich are also gratefully acknowledged.

[1]See, for example, R. C. Baetzold and J. F. Hamilton, Prog. Solid State Chem. (in press).
[2]M. G. Mason and R. C. Baetzold, J. Chem. Phys. 64, 271 (1976).
[3]R. C. Baetzold, J. Appl. Phys. 47, 3799 (1976).
[4]K. S. Liang, W. R. Salaneck, and I. S. Aksay, Solid State Commun. 19, 329 (1976).
[5]M. G. Mason, L. J. Gerenser, and S.-T. Lee, Phys. Rev. Lett. 39, 288 (1977).
[6]Y. Takasu, R. Unwin, B. Tesche, and A. M. Bradshaw, Surf. Sci. 77, 219 (1978); R. Unwin and A. M. Bradshaw, Chem. Phys. Lett. 58, 58 (1978).
[7]W. F. Egelhoff, Jr., and G. G. Tibbetts, Phys. Rev. B 19, 5028 (1979); Solid State Commun. 29, 53 (1979).
[8]J. F. Hamilton and R. C. Baetzold, Science 205, 1213 (1979).
[9]G. Apai, J. F. Hamilton, J. Stohr, and A. Thompson, Phys. Rev. Lett. 43, 165 (1979).
[10]M. K. Bahl, S. C. Tsai, and Y. W. Chung, Phys. Rev. B 21, 1344 (1980).
[11]H. Roulet, J.-M. Mariot, G. Dufour, and C. F. Hague, J. Phys. F 10, 1025 (1980).
[12]M. G. Mason, S.-T. Lee, and G. Apai, Chem. Phys. Lett. 76, 51 (1980).
[13]J. F. Hamilton, G. Apai, S.-T. Lee, and M. G. Mason, in *Growth and Properties of Metal Clusters,* edited by J. Bourdon (Elsevier, Amsterdam, 1980), p. 387.
[14]R. C. Baetzold, M. G. Mason, and J. F. Hamilton, J. Chem. Phys. 72, 366 (1980); 72, 6820 (1980).
[15]L. Oberli, R. Monot, H. J. Mathieu, D. Landolt, and J. Buttet, Surf. Sci. 106, 301 (1981).
[16]S.-T. Lee, G. Apai, M. G. Mason, R. Benbow, and Z. Hurych, Phys. Rev. B 23, 505 (1981).
[17]G. Apai, S.-T. Lee, and M. G. Mason, Solid State Commun. 37, 213 (1981).
[18]J. M. Burkstrand, J. Vac. Sci. Technol. 20, 440 (1982), and references therein.
[19]M. G. Mason, S.-T. Lee, G. Apai, R. F. Davis, D. A Shirley, A. Franciosi, and J. H. Weaver, Phys. Rev. Lett. 47, 730 (1981).
[20]J. C. Slater and K. H. Johnson, Phys. Today 27 (10),34 (1974).
[21]J. F. Hamilton and P. C. Logel, Thin Solid Films 23, 89 (1974).
[22]J. F. Hamilton, P. C. Logel, and R. C. Baetzold, Thin Solid Films 32, 233 (1976).
[23]J. F. Hamilton, J. Vac. Sci. Technol. 13, 319 (1976).
[24]J. F. Hamilton, D. R. Preuss, and G. Apai, Surf. Sci. 106, 146 (1981), and private communication.
[25]B. Johansson and N. Mårtensson, Phys. Rev. 21, 4427 (1980).
[26]R. E. Watson, J. Hudis, and M. L. Perlman, Phys. Rev. B 4, 4139 (1971).
[27]R. E. Watson and M. L. Perlman, Struct. Bonding (Berlin) 24, 83 (1975).
[28]A. R. Williams and N. D. Lang, Phys. Rev. Lett. 40, 954 (1978).
[29]K. S. Schönhammer and O. Gunnarsson, Solid State Commun. 23, 691 (1977); 26, 147 (1978); Z. Phys. B 30, 297 (1978).
[30]J. C. Fuggle, M. Campagna, Z. Zolnierek, and R. Lässer, Phys. Rev. Lett. 45, 1597 (1980).
[31]P. Ascarelli, M. Cini, G. Missoni, and N. Nistico, J. Phys. (Paris) Colloq. 2, 125 (1977); E. J. Aitken, M. K. Bahl, K. D. Bomben, J. K. Gimzewski, G. S. Nolan, and T. D. Thomas, J. Am. Chem. Soc. 102, 4873 (1980).
[32]T. D. Thomas, J. Electron Spectrosc. Relat. Phenom. 20, 117 (1980).
[33]R. M. Friedman, J. Hudis, M. L. Perlman, and R. E. Watson, Phys. Rev. B 8, 2433 (1973).
[34]L. F. Mattheiss and R. E. Dietz, Phys. Rev. B 22, 1663 (1980).
[35]N. E. Christensen, J. Phys. F 8, L51 (1978); C. D. Gelatt, Jr., and H. Ehrenreich, Phys. Rev. B 10, 398 (1974).
[36]J. H. S. Scofield, J. Electron Spectrosc. Relat. Phenom. 8, 129 (1976).
[37]M. Brown, R. E. Peierls, and E. A Stern, Phys. Rev. B 15, 738 (1977).
[38]F. W. Lytle, J. Catal. 43, 376 (1976).
[39]D. R. Preuss and J. F. Hamilton (unpublished).
[40]S. Hüfner and G. K. Wertheim, Phys. Rev. B 11, 678 (1975); G. K. Wertheim and L. R. Walker, J. Phys. F 6, 2297 (1976); G. K. Wertheim and P. H. Citrin, in *Topics in Applied Physics,* edited by M. Cardona and L. Ley (Springer, New York, 1978), Vol. 26, p. 197.
[41]R. A. Gibbs, N. Winograd, and V. Y. Young, J. Chem. Phys. 72, 4799 (1980).
[42]T. K. Sham, M. L. Perlman, and R. E. Watson, Phys. Rev. B 19, 539 (1979); 20, 3552 (1979); 21, 1457 (1980); R. E. Watson and M. L. Perlman, Phys. Scr. 21, 527

(1980); T. S. Chou, M. L. Perlman, and R. E. Watson, Phys. Rev. B 14, 3248 (1976).

[43]N. J. Shevchik, J. Phys. F 5, 1860 (1975).

[44]J. A. Nicholson, J. D. Riley, R. C. G. Leckey, J. G. Jenkin, J. Liesegang, and J. Azoulay, Phys. Rev. B 18, 2561 (1978); J. A. Nicholson, J. D. Riley, R. C. G. Leckey, J. G. Jenkin, and J. Liesegang, J. Electron Spectrosc. Relat. Phenom. 15, 95 (1979).

[45]K. Tamura, J. Fukushima, H. Endo, K. Kishi, S. Ikeda, and S. Minomura, J. Phys. Soc. Jpn. 36, 565 (1974).

[46]P. Steiner, S. Hüfner, N. Mårtensson, and B. Johansson, Solid State Commun. 37, 73 (1981).

[47]Actual splitting depends on photon energy and resolution, but in all cases agreement between the cluster and alloys is excellent.

[48]C. J. Ballhausen and H. B. Gray, *Molecular Orbital Theory* (Benjamin, New York, 1965).

[49]V. L. Moruzzi, A. R. Williams, and J. F. Janak, Phys. Rev. B 10, 4856 (1974).

[50]J. Friedel, J. Phys. F 3, 785 (1973).

[51]R. C. Baetzold, J. Chem. Phys. 68, 555 (1978); 82, 738 (1978).

[52]The linear dependent of $\Delta E$ on alloy concentration is also observed in other alloy systems. See, for example, N. Mårtensson, R. Nyholm, and B. Johansson, Phys. Rev. Lett. 45, 754 (1980); see also Ref. 53.

[53]N. Mårtensson, R. Nyholm, J. Calén, J. Hedman, and B. Johansson, Phys. Rev. B 24, 1725 (1981).

[54]T. M. Duc, C. Guillot, Y. Lassailly, J. Lecante, Y. Jugnet, and J. C. Vedrine, Phys. Rev. Lett. 43, 789 (1979); J. F. van der Veen, F. J. Himpsel, and D. E. Eastman, *ibid.* 44, 189 (1980); 44, 553 (1980); J. F. van der Veen, P. Heimann, F. J. Himpsel, and D. E. Eastman, Solid State Commun. 37, 555 (1981); P. Heimann, J. F. van der Veen, and D. E. Eastman, *ibid.* 38, 595 (1981); R. C. Baetzold, G. Apai, E. Shustorovich, and R. Jaeger, Phys. Rev. B 26, 4022 (1982).

[55]P. H. Citrin. G. K. Wertheim, and Y. Baer, Phys. Rev. Lett. 41, 1425 (1978).

[56]P. Steiner and S. Hüfner, Solid State Commun. 37, 279 (1981).

[57]The interaction between neighbors discussed here is similar to that described in Ref. 49 to explain the bandwidth in intermetallic compounds.

[58]R. A. Pollak, S. Kowalczyk, L. Ley, and D. A. Shirley, Phys. Rev. Lett. 29, 274 (1972).

[59]V. L. Moruzzi, J. F. Janak, and A. E. Williams, *Calculated Electronic Properties of Metals* (Pergamon, New York, 1978); M. G. Ramchamdani, in *Proceedings of the Nuclear Physics Solid-State Physics Symposium,* (Physics Committee Dept. Atomic Energy, Bombay, India, 1972), Vol. 16, p. 49; S. Pendyala, M. M. Pant, and B. Y. Tong, Can. J. Phys. 49, 2633 (1971); J. Chowdhuri, P. Chatterjee, and S. Chatterjee, J. Phys. F 9, 683 (1979); M. A. E. A. Ament and A. R. de Vroomen, *ibid.* 4, 1359 (1974); P. Kay and J. A. Reissland *ibid.* 6, 1503 (1976); L. M. Falicov and P. J. Lin, Phys. Rev. 141, 562 (1966); J. D. Joannopoulos, M. Schlüter, and M. L. Cohen, Phys. Rev. B 11, 2186 (1975).

[60]The indicated position of the Au 5*d* levels is that measured for Au on C and Cd where the substrate orbitals are weak enough that the shape of the Au valence band can be determined accurately.

[61]M. C. Desjonqueres, D. Spanjaard, Y. Lassailly, and C. Guillot, Solid State Commun. 34, 807 (1980).

[62]A. Rosengren and B. Johansson, Phys. Rev. B 22, 3706 (1980).

[63]J. B. Mann, Los Alamos Scientific Laboratory Report No. LASL-2690 (unpublished).

[64]P. Steiner and S. Hüfner, Acta Metall. 29, 1885 (1981); V. Kumar, D. Tománek, and K. H. Bennemann, Solid State Commun. 39, 987 (1981).

[65]R. Hultgren, R. L. Orr, P. D. Anderson, and K. K. Kelley, *Selected Values of Thermodynamic Properties of Metal Alloys* (Wiley, New York, 1963).

[66]A. R. Miedema, J. Less-Common Met. 32, 117 (1973); 46, 67 (1976); Philips Tech. Rev. 36, 217 (1976); Physica B 100, 1 (1980); A. R. Miedema, R. Boom, and F. R. De Boer, J. Less-Common Met. 41, 283 (1975); R. Boom, F. D. De Boer, and A. R. Miedema, *ibid.* 45, 237 (1976); A. R. Miedema, F. R. DeBoer, and R. Boom, CALPHAD 1, 341 (1977).

[67]W. F. Egelhoff, Jr., J. Vac. Sci. Technol. 20, 668 (1982), and private communication.

[68]K. S. Kim and N. Winograd, Chem. Phys. Lett. 30, 91 (1975).

[69]The semiempirical model of Miedema and co-workers has been criticized for the physical interpretation given the parameters: D. G. Pettifor, Solid State Commun. 28, 621 (1978); Phys. Rev. Lett. 42, 846 (1979); A. R. Williams, C. D. Gelatt, Jr., and V. L. Moruzzi, Phys. Rev. Lett. 44, 429 (1980). However, the general ability of the model to calculate accurate heats of solutions is widely accepted. Unfortunately, some of the poorest results are obtained for systems containing Hg, which is the $Z+1$ state of Au. The calculated value of $E$(Hg; Au) is 0.28 eV, compared to experimental values which range from 0.07 eV [H.W. Rayson and W. A. Alexander, Acta Metall. 8, 833 (1960)] to $-0.11$ eV (Ref. 65). In view of the large discrepancies in experimental values and for consistency, we have chosen to use calculated values throughout this work.